# Global Transport Modeling of Impact Released Volatiles from Lunar Soils

O.J. Tucker[1], J. McLain[1], W.M. Farrell[1], D.M. Hurley[2] ([1]NASA Goddard Space Flight Center, 20771, [2]Greenbelt, Maryland, Johns Hopkins University Applied Physics Lab, 20723, Laurel, Maryland)

**Introduction:** Water products ($H_2O$, OH, H) have been observed unambiguously throughout the lunar surface both within permanently shadowed regions (PSRs) (1–3) and widespread throughout sunlight regions (4–6). Both surface spectra obtained by Chandrayaan-I Moon Mineralogy Mapper ($M^3$) and the Lunar Reconnaissance Orbiter Lyman-Alpha Mapping Project LRO-LAMP indicate that surface hydration varies with time of day. However observations of water products, specifically OH/$H_2O$, in the exosphere are sparse. Therefore, connecting water products in the exosphere to known surface reservoirs (hydrogen within the top monolayers of grains and within PSRs) is not well characterized. Here we examine the augmentation of the water exosphere during meteoroid impacts using preliminary results of evolved gases produced during flash desorption experiments of the Apollo Soil 78421 tracked in a global Monte Carlo exosphere model.

Recently, the Lunar Atmosphere and Dust Environment Explorer Neutral Mass Spectrometer (LADEE NMS) measurements of OH/$H_2O$ have been correlated to meteoroid streams which produced temporal median densities of 22.8 mol cm$^{-3}$ (7). However, for the steady state exosphere produced from desorption processes LADEE-NMS data is indicative of a much lower limit of 0.69 cm$^{-3}$. This observation is inconsistent with inferred desorption rates inferred from the temporal variation of surface hydration observed by LRO-LAMP (8) and $M^3$ (9, 10). Modeling the distribution of OH/$H_2O$ in the exosphere produced by thermal desorption and micrometeoroid impact allows us to predict observational signatures to decipher the inferences.

Secondly, $H_2$ is the dominant hydrogen bearing to have been observed in the steady-state lunar exosphere. LRO-LAMP measurements were used to derive $H_2$ surface densities of 1000 ± 500 cm$^{-3}$ and 1400 ± 500 cm$^{-3}$ the dusk and dawn terminators, respectively (11), and the Chandrayaan Chandra Altitudinal Composition Explorer (CHACE) mass spectrometer measured $H_2$ abundances in the magnetotail consistent with surface densities of 500 – 800 cm$^{-3}$ over latitudes of 20 – 80 degrees, respectively (12). Both measurements are consistent with the $H_2$ exosphere being derived from the solar wind (13, 14). Molecular hydrogen is also a significant product released during impacts as indicated by the Lunar Crater Observation and Sensing Satellite (LCROSS) experiment (13, 15), and in the preliminary flash desorption experiments shown in Figure 1. Crider et al. (2000) showed that micrometeoroid impacts are an insufficient source to produce the averaged LAMP observations. Here, we build on this effort by examining the variation of exospheric $H_2$ densities augmented with micrometeoroid impacts over the lunar cycle.

Even less understood are the contribution of exospheric water products to cold traps. Of considerable interest is how and of what form volatiles ($H_2O$ vs. $H_2$) are delivered to the PSRs. The LCROSS impact released a host of volatile compounds including $H_2$, $H_2O$, $CO_2$, OH, $H_2S$, $CH_4$, and $SO_2$ within the Cabeus crater (2, 15). Modeling the concomitant composition of the exosphere produced during micrometeoroid impacts will provide further insight into this process. With the Monte Carlo model we can characterize the contribution of volatiles that encounter cold traps.

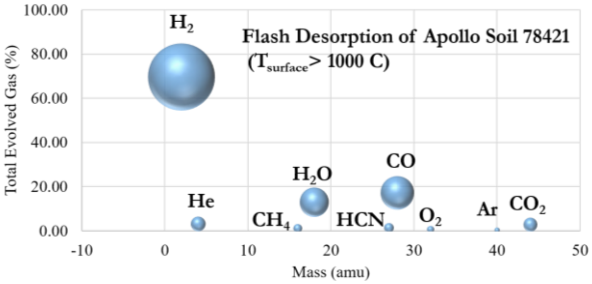

**Figure 1:** Fraction of desorbed gas from flash heating of Apollo Soil 78421 at temperatures > ~1300 K. (Preliminary Results)

**Methods:** Experimentally derived mass spectra (Figure 1) will be used in a global Monte Carlo model to track the evolution of meteoroid induced volatized gases. The influence of the released volatiles on the background solar wind atmosphere will be examined. The solar wind source will depended on the local zenith about noon, and we will adopt the micrometeoroid source rates from Crider et al. (200) and references therein. Volatilized gases to be track will include $H_2$, $H_2O$, CO and He assuming a degassing temperature of $T$ = 1300 K (Maxwellian). The model will simulate the evolution of the gases by tracking losses to escape and polar cold traps. The probability to be loss to a cold trap is considered using the fractional area of PSRs, 7500 km$^2$ and 6500 km$^2$, within 9 degrees of the northern and southern poles, respectively. In the model we will assume full thermal accommodation for molecules that impact the surface with 100 % sticking of $H_2O$ on at surface temperatures < 270 K and $H_2$ is assumed to only stick within PSRs. The lifetime against photodestruction of molecules in the exosphere are adopted from Huebner et al. (2015) (16).

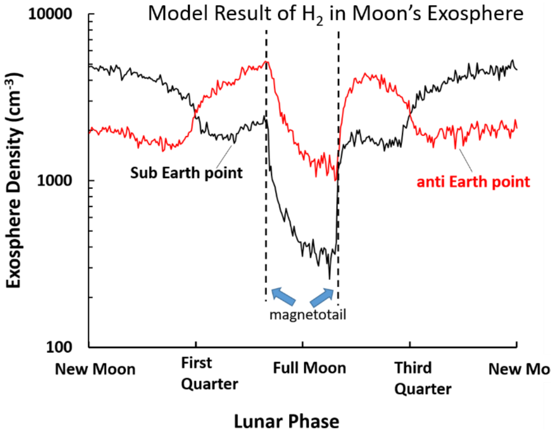

**Figure 2:** Modeled $H_2$ exospheric density at sub and anti Earth points. The dashed line indicated the average time spent in the magnetotail.

**Results:** Our presentation will review the temporal and global evolution of gases after meteoroid impact, and when applicable compare that distribution to exospheric densities derived from solar wind implantation (e.g. He, $H_2$, OH subsequent *re-combinative desorption*) and thermal desorption (e.g. $H_2O$). Figure 2 shows an example of the temporal evolution of the $H_2$ exospheric surface density produced by solar wind implantation at the sub Earth and anti-Earth points over the lunar cycle. For example, we will predict the exospheric response to impacts while in the magnetotail when the solar wind source is reduced. Tracking the evolution of impact released volatiles over the lunar cycle will enable us to determine expected observational signatures which can be used to test theory. Likewise, we will present results on the escape and PSR area accumulation rates for the various species tracked by the simulations.

**References:**

1. Hayne PO, Hendrix A, Sefton-Nash E, Siegler MA, Lucey PG, et al. 2015. *Icarus*. 255:58–69
2. Colaprete A, Schultz P, Heldmann J, Wooden D, Shirley M, et al. 2010. *Science (80-. )*. 330(6003):463–68
3. Feldman WC, Lawrence DJ, Elphic RC, Barraclough BL, Maurice S, et al. 2000. *J. Geophys. Res. E Planets*. 105(E2):4175–95
4. McCord TB, Taylor LA, Combe JP, Kramer G, Pieters CM, et al. 2011. *J. Geophys. Res. E Planets*. 116(4):1–22
5. Wöhler C, Grumpe A, Berezhnoy AA, Shevchenko V V. 2017. *Sci. Adv*. 3(9):1–11
6. Honniball CI, Lucey PG, Li S, Shenoy S, Orlando TM, et al. 2020. *Nat. Astron.*
7. Benna M, Hurley DM, Stubbs TJ, Mahaffy PR, Elphic RC. 2019. *Nat. Geosci*. 12(5):333–38
8. Hendrix AR, Hurley DM, Farrell WM, Greenhagen BT, Hayne PO, et al. 2019. *Geophys. Res. Lett*. 46(5):2417–24
9. Li S, Milliken RE. 2017. *Sci. Adv*. 3(9):1–12
10. Jones BM, Sarantos M, Orlando TM. 2020. *Astrophys. J*. 891(2):L43
11. Cook JC, Stern SA, Feldman PD, Gladstone GR, Retherford KD, Tsang CCC. 2013. *Icarus*. 225(1):681–87
12. Thampi S V., Sridharan R, Das TP, Ahmed SM, Kamalakar JA, Bhardwaj A. 2015. *Planet. Space Sci*. 106:142–47
13. Crider DH, Vondrak RR. 2000. *J. Geophys. Res. E Planets*. 105(E11):26773–82
14. Tucker OJ, Farrell WM, Killen RM, Hurley DM. 2019. *J. Geophys. Res. Planets*. 124(2):
15. Hurley DM, Gladstone GR, Stern SA, Retherford KD, Feldman PD, et al. 2012. *J. Geophys. Res. E Planets*. 117(2):1–15
16. Huebner WF, Mukherjee J. 2015. *Planet. Space Sci.*

**Acknowledgements:** The authors acknowledge support for NASA internal science funding GSFC FLaRE and EIMM programs.